Superexchange in the cuprates

Henk Eskes* and John H. Jefferson
Defence Research Agency, Electronics Sector, St. Andrews Road, Great Malvern, Worcestershire WR14 3PS, England
(Received 8 February 1993)

It is shown that the usual three-center cation-anion-cation model or fourth-order pertrubation expression (in the Cu-O hopping parameter t_{pd}) does not give a useful (even qualitative) estimate for the superexchange J, even though, by coincidence, it predicts a magnitude that is reasonable. There are two additional contributions, both due to the oxygen-oxygen hopping t_{pp}, which are estimated to be responsible for about $\frac{2}{3}$ of the total exchange interaction. The first causes a strong enhancement of the usual fourth-order J and is conventional in the sense that it goes like $1/U$ for a large on-site Coulomb interaction U on copper and oxygen, and is always antiferromagnetic (AFM). Its importance is due to a large prefactor in the perturbation series in t_{pp}/Δ, where Δ is the charge-transfer energy. The second AFM term is of a topological nature in the sense that its sign is determined by the signs of the different hopping parameters and the arrangement of the Cu and O sites in the CuO_2 planes. This term does *not* involve doubly occupied sites, and is a consequence of the extra degrees of freedom formed by the oxygen $2p$ orbitals. Starting from the three-band model, these two effects are examined by means of fifth-order perturbation theory and perturbation theory that involves oxygen bands explicitly. The results are compared with numerical estimates of J from finite-size clusters.

I. INTRODUCTION

One of the main problems in understanding the normal-state as well as the superconducting properties of the cuprate high-T_c superconductors and their stoichiometric parent compounds is the presence of strong antiferromagnetic couplings between the spins, which are a consequence of the strong Coulomb interactions on the Cu sites. These interactions cause the undoped materials, such as La_2CuO_4, to be insulators of the charge-transfer type, with a surprisingly strong superexchange interaction between the predominantly Cu spins. Measurements show that these strong spin interactions are still present in the doped superconducting materials. These observations have led to the proposal of attractive interactions between strongly renormalized charge carriers caused by the spin background or even a breakdown of Fermi-liquid theory.[1]

The two-dimensional Heisenberg model seems to give a consistent description of the (low-energy) excitation spectrum of the insulating La_2CuO_4 compound.[2,3] The Hamiltonian is given by

$$H = J \sum_{\langle i,j \rangle} \mathbf{S}_i \cdot \mathbf{S}_j \ . \tag{1}$$

Measurements of the spin-wave velocity and the temperature dependence of the correlation length interpreted in terms of this model are in good agreement with each other and with a moment analysis of the Raman B_{1g} spectrum, and all lead to a value for J of about 0.13 eV.[4–6] The situation concerning the measured magnetic moment is less clear.[7] To understand other experimental data, such as the staggered magnetization and susceptibility, a weak interlayer coupling $J' \ll J$ as well as a Dzyaloshinskii-Moriya spin-spin interaction are introduced in addition to Eq. (1). Longer-range spin interactions, such as next-nearest-neighbor interactions, are thought to be small,[8] although some authors claim that four-site spin interactions are of importance.[9,10]

Our starting point will be the three-band model, introduced by Emery shortly after the discovery of the high-T_c compounds.[11] An important parameter in this model is the direct oxygen-oxygen hopping t_{pp}. Band-structure calculations[12] predict this value to be large ($t_{pp} \approx t_{pd}/2$, where t_{pd} is the Cu-O hybridization matrix element between the Cu $d_{x^2-y^2}$ and an oxygen p_σ orbital). This is consistent with an oxygen bandwidth of around 4–5 eV as seen in various high-energy spectroscopy experiments. For the low-energy excitation spectrum of the insulator and for estimating J, the other $3d$ bands are not likely to be of much importance. Comparison of a calculation of J for a Cu_2O_7 cluster for the three-band model with parameter values listed in Ref. 10 give a difference in J of no more than 1.5% as compared with the result for a calculation which includes all five $3d$ orbitals on Cu with its full $3d$ multiplet structure, as well as all three O $2p$ orbitals with its $2p$ multiplet structure.[13,14]

Starting from the three-band Emery model, one obtains the following expression for the superexchange in fourth order:

$$J = \frac{4t_{pd}^4}{(\Delta + U_{pd})^2} \left[\frac{1}{U_d} + \frac{2}{2\Delta + U_p} \right] . \tag{2}$$

Here U_d, U_p, and U_{pd} represent the on-site interaction on Cu, O, and the intersite Coulomb interaction between Cu and O holes, respectively. Δ is the charge-transfer energy or the energy difference between the Cu $3d$ and O $2p$ levels. Since this expression involves only two neighboring Cu sites and their intermediate oxygen, it is equivalent to

the three-center cation-anion-cation model expanded to fourth order. This formula is often used to estimate the superexchange from the parameters in the three-band model or to estimate an unknown parameter in the three-band model using the measured value of J. Note that this fourth-order expression for the superexchange does *not* depend on the O-O hopping term t_{pp}, despite its presence in the original Hamiltonian [Eq. (6), next section].

In this paper we will show that expression (2) is inadequate. We point out that for realistic values of the parameters in the cuprates, the perturbation expansion is slowly convergent and therefore expression (2) *overestimates* J. However, as we will show later, expression (2) strongly *underestimates* J, since it neglects the effects of t_{pp}. These two effects cancel each other for a large part. It is therefore a coincidence that the fourth-order expression (2) gives a reasonable estimate of the superexchange.

The purpose of this paper is to identify the different contributions to the superexchange, starting from a general three-band model, and not in the first place to find a realistic estimate. In the literature there have been various estimates of J using exact cluster results.[13–16] Of course, these calculations do not suffer from the above-mentioned problems of the fourth-order expression. However, they do not give a real insight into which different contributions are responsible for the unusually large J value experimentally observed.

Both Eq. (2) and the original superexchange theory of Anderson[17] (giving $J=4t^2/U$) have the common feature that the spin interaction goes as $1/U$. However, we will show that for the three-band model the exchange does *not* vanish if both U_d and $U_p \to \infty$. The remaining interaction is in fact quite large and contributes a substantial portion of the total exchange.

The paper is organized in the following way. In the next section, we will briefly review the derivation of the fourth-order expression (2). In Sec. III we will extend this formula up to fifth order, in which both effects mentioned above will begin to occur. In Sec. IV we consider a set of Cu atoms coupling to an oxygen band (neglecting the interactions U_p). In this way we arrive at an expression for J which is fourth order in t_{pd}, but contains the effect of t_{pp} up to infinite order. The above approaches serve to clarify the different contributions to J and the importance of t_{pp}, but are not appropriate for making an actual estimate of the superexchange interaction. In Sec. V we will more quantitatively address the relative importance of the different contributions to J by numerically solving clusters containing two Cu sites.

II. THREE-CENTER CATION-ANION-CATION MODEL

In this section we will briefly review superexchange interactions and in particular the derivation of the fourth-order expression for the three-band model.

A theory for superexchange interactions between metal ions in a nonmagnetic host was developed in 1959 by Anderson[17] (for a review, see Ref. 18). His starting point is the **k**-dependent band structure of the system. If the bands of mainly metal character are narrow, it is a better starting point to Fourier transform these running waves to real-space Wannier functions centered on the metal sites and in zeroth order neglect the hopping between them.

If the repulsion U between two electrons (holes) in the same Wannier state is much larger than the hopping $b_{i,j}$ between neighboring Wannier states, charge fluctuations will be strongly reduced and a gap will open up in the one-particle spectrum. Virtual hopping of particles to neighboring Wannier orbitals will lift the remaining spin degeneracy and give rise to a superexchange interaction which is second order in $b_{i,j}$.

The above reasoning leads to a single-band Hubbard model

$$H=\sum_{i,j,\sigma} b_{i,j} w^{\dagger}_{i,\sigma} w_{j,\sigma} + U \sum_{i} n_{i,\uparrow} n_{i,\downarrow} \ . \tag{3}$$

Because the exchange interaction occurs in second order, we can consider two neighboring sites, say, sites 1 and 2. The 2×2 Hamilton matrix and corresponding singlet states are

$$\begin{bmatrix} 0 & 2b_{1,2} \\ 2b_{1,2} & U \end{bmatrix} \text{ and } \begin{cases} \frac{1}{\sqrt{2}}(w^{\dagger}_{1,\uparrow} w^{\dagger}_{2,\downarrow} + w^{\dagger}_{2,\uparrow} w^{\dagger}_{1,\downarrow})|\text{vac}\rangle \\ \frac{1}{\sqrt{2}}(w^{\dagger}_{1,\uparrow} w^{\dagger}_{1,\downarrow} + w^{\dagger}_{2,\uparrow} w^{\dagger}_{2,\downarrow})|\text{vac}\rangle \ . \end{cases} \tag{4}$$

The remaining states form a triplet of zero energy. The superexchange is simply the energy difference between the triplet and lowest singlet state, giving

$$J_{i,j}=\frac{4b^2_{i,j}}{U} \tag{5}$$

in second order.

This kinetic exchange is always antiferromagnetic and is due to the extra phase space which lowers the energy of the singlet state relative to the triplet state. Note that this procedure is different from a perturbation approach which starts from atomic ($3d$) orbitals. The Wannier orbitals w_i obtained in this way can and will be of substantial host character, and the energy will be lowered considerably as compared to the energy of the (embedded) atomic orbitals. Thus most of the metal-host hybridization is already contained in the orbitals w_i,[20] and in this sense the approach is superior with respect to atomic perturbation theory. In the case of copper oxides, this means roughly that $w_{i,\sigma}=\alpha d_{i,\sigma}+\beta P_{i,\sigma}$, where d annihilates holes in atomic $d_{x^2-y^2}$ orbitals and P annihilates holes in O $2p$ orbitals of $d_{x^2-y^2}$ symmetry centered around the same Cu atom.

The active component in the cuprate materials are planes made out of CuO_2 unit cells forming a square lattice. The three-band model, describing the Cu $3d_{x^2-y^2}$ and the two oxygen p_σ orbitals, is given by[11]

$$H=\varepsilon_d \sum_{i,\sigma} d^\dagger_{i,\sigma} d_{i,\sigma} + (\varepsilon_d+\Delta) \sum_{i,\sigma} p^\dagger_{i,\sigma} p_{i,\sigma} + \sum_{\langle i,j\rangle\sigma} t_{i,j} (d^\dagger_{i,\sigma} p_{j,\sigma} + \text{H.c.}) + \sum_{\langle i,j\rangle\sigma} t'_{i,j} (p^\dagger_{i,\sigma} p_{j,\sigma} + \text{H.c.})$$
$$+ U_d \sum_i d^\dagger_{i,\uparrow} d_{i,\uparrow} d^\dagger_{i,\downarrow} d_{i,\downarrow} + U_p \sum_i p^\dagger_{i,\uparrow} p_{i,\uparrow} p^\dagger_{i,\downarrow} p_{i,\downarrow} + U_{pd} \sum_{\langle i,j\rangle,\sigma,\sigma'} d^\dagger_{i,\sigma} d_{i,\sigma} p^\dagger_{j,\sigma'} p_{j,\sigma'} , \tag{6}$$

where p annihilates holes in one of the two O $2p_\sigma$ orbitals. t describes the Cu-O hopping and is equal to $\pm t_{pd}$, the sign depending on the relative phase of the overlapping $d_{x^2-y^2}$ and $2p_\sigma$ lobes. t' describes nearest-neighbor O-O hopping and is equal to $\pm t_{pp}$. The other terms describe the on-site repulsion between two Cu holes, two O holes, and the intersite repulsion between a hole on Cu and a hole on a nearest-neighbor oxygen, respectively. The above Hamiltonian will be our starting point for the rest of this paper. Note that the d and p labels refer to effective orbitals, and for instance the p orbital will in reality have a considerable component of Cu $4s,p$ character. We remark that although Eq. (6) is thought to give a rather accurate description of the states around the chemical potential, many approximations have been made that could be of importance for the exchange interaction. For instance, explicit electron-hole excitations (Cu $4sp$ bands) are absent in Eq. (6), the inclusion of other oxygen $2p$ orbitals as well as the $4sp$ bands will modify the oxygen-band energies, and all intersite Coulomb and exchange matrix elements (except for U_{pd}) are neglected in the above equation.

The fourth-order expression for J (Refs. 15 and 21–24) can be derived using canonical perturbation theory or Rayleigh-Schrödinger perturbation theory.[25–28] Since four hops involve only two neighboring Cu sites and the intermediate oxygen, we can derive the expression from a Cu_2O cluster (three-center cation-anion-cation model). Starting from two holes localized on the two coppers (d_1 and d_2), we can generate the other states by applying the hopping part of the Hamiltonian [Eq. (6)]. The singlet Hamilton matrix and corresponding states are

$$\begin{bmatrix} 0 & \sqrt{2}t_{pd} & 0 & 0 \\ \sqrt{2}t_{pd} & \Delta+U_{pd} & 2t_{pd} & \sqrt{2}t_{pd} \\ 0 & 2t_{pd} & U_p+2\Delta & 0 \\ 0 & \sqrt{2}t_{pd} & 0 & U_d \end{bmatrix} \text{ and } \begin{cases} \frac{1}{\sqrt{2}}(d^\dagger_{1,\uparrow} d^\dagger_{2,\downarrow} + d^\dagger_{2,\uparrow} d^\dagger_{1,\downarrow})|\text{vac}\rangle , \\ \frac{1}{2}(p^\dagger_\uparrow d^\dagger_{2,\downarrow} + d^\dagger_{1,\uparrow} p^\dagger_\downarrow + p^\dagger_\uparrow d^\dagger_{1,\downarrow} + d^\dagger_{2,\uparrow} p^\dagger_\downarrow)|\text{vac}\rangle , \\ p^\dagger_\uparrow p^\dagger_\downarrow |\text{vac}\rangle , \\ \frac{1}{\sqrt{2}}(d^\dagger_{1,\uparrow} d^\dagger_{1,\downarrow} + d^\dagger_{2,\uparrow} d^\dagger_{2,\downarrow})|\text{vac}\rangle , \end{cases} \tag{7}$$

whereas for the triplet we get

$$\begin{bmatrix} 0 & \sqrt{2}t_{pd} \\ \sqrt{2}t_{pd} & \Delta+U_{pd} \end{bmatrix} \text{ and } \begin{cases} \frac{1}{\sqrt{2}}(d^\dagger_{1,\uparrow} d^\dagger_{2,\downarrow} - d^\dagger_{2,\uparrow} d^\dagger_{1,\downarrow})|\text{vac}\rangle , \\ \frac{1}{2}(p^\dagger_\uparrow d^\dagger_{2,\downarrow} + d^\dagger_{1,\uparrow} p^\dagger_\downarrow - p^\dagger_\uparrow d^\dagger_{1,\downarrow} - d^\dagger_{2,\uparrow} p^\dagger_\downarrow)|\text{vac}\rangle . \end{cases} \tag{8}$$

Again, the difference between singlet and triplet is just the doubly occupied configurations, with energies U_d and U_p. Expanding the two ground-state energies to fourth order gives Eq. (2). Of course, one does not have to approximate J up to fourth order, but one can find J directly as the energy difference of the ground states obtained by solving the singlet and triplet matrices numerically.

The first term in Eq. (2) can be understood with the original superexchange theory,[17] where $t_{pd}^2/(\Delta+U_{pd})$ is identified as the perturbation-theory estimate of the hopping b between the Wannier orbitals w, and the on-site repulsion is $\approx U$. The second term was derived by Geertsma[21] and involves an intermediate state with two holes on oxygen. This extra term can be neglected in the extreme Mott-Hubbard case ($\Delta \gg U$), but is important for charge-transfer insulators ($U \geq \Delta$). Zaanen and Sawatzky[23] have shown that the full expression [Eq. (2)] leads to a trend in the Néel temperature of the transition-metal monoxides series from Mn to Ni which is consistent with experiment, improving on Anderson's original results based on the first term only.

Stechel and Jennison[15] argued that the exchange part of the Cu-O interaction U_{pd} is important and gives rise to a ferromagnet correction[17] to Eq. (2). This ferromagnetic term is second order in the hopping. Calling the intersite exchange integral K and neglecting doubly occupied

configurations, the singlet matrix and corresponding states are given by

$$\begin{bmatrix} 0 & \sqrt{2}t_{pd} \\ \sqrt{2}t_{pd} & \Delta+U_{pd}-K \end{bmatrix}$$

and

$$\begin{cases} \frac{1}{\sqrt{2}}(d^\dagger_{1,\uparrow}d^\dagger_{2,\downarrow}+d^\dagger_{2,\uparrow}d^\dagger_{1,\downarrow})|\text{vac}\rangle , \\ \frac{1}{2}(p^\dagger_\uparrow d^\dagger_{2,\downarrow}+d^\dagger_{1,\uparrow}p^\dagger_\downarrow+p^\dagger_\uparrow d^\dagger_{1,\downarrow}+d^\dagger_{2,\uparrow}p^\dagger_\downarrow)|\text{vac}\rangle , \end{cases} \tag{9}$$

whereas for the triplets we get

$$\begin{bmatrix} 0 & \sqrt{2}t_{pd} \\ \sqrt{2}t_{pd} & \Delta+U_{pd}+K \end{bmatrix}$$

and

$$\begin{cases} \frac{1}{\sqrt{2}}(d^\dagger_{1,\uparrow}d^\dagger_{2,\downarrow}-d^\dagger_{2,\uparrow}d^\dagger_{1,\downarrow})|\text{vac}\rangle , \\ \frac{1}{2}(p^\dagger_\uparrow d^\dagger_{2,\downarrow}+d^\dagger_{1,\uparrow}p^\dagger_\downarrow-p^\dagger_\uparrow d^\dagger_{1,\downarrow}-d^\dagger_{2,\uparrow}p^\dagger_\downarrow)|\text{vac}\rangle . \end{cases} \tag{10}$$

The energy difference between the two ground-state energies gives a ferromagnetic exchange interaction

$$J\approx\frac{4t_{pd}^2}{(\Delta+U_{pd})^2}K . \tag{11}$$

For $K\approx-0.22$ eV as estimated by Stechel and Jennison, this is a large correction and should be included in a realistic estimate of J.

III. FIFTH-ORDER RAYLEIGH-SCHRÖDINGER PERTURBATION THEORY

In this section we will show that both corrections mentioned in the Introduction first occur in fifth-order in perturbation theory. We will use the Rayleigh-Schrödinger (RS) (Ref. 29) formulation of perturbation theory, which leads to an effective Hamiltonian operating in the (spin-degenerate) space of one hole per copper.

The zeroth-order wave functions (2^N-fold-degenerate ground manifold) are

$$|\sigma_1\cdots\sigma_N\rangle=\prod_{i=1}^{N}d^\dagger_{i,\sigma_i}|\text{vac}\rangle , \tag{12}$$

where the product ranges over Cu-site indices. The RS effective Hamiltonian for this set of states, up to fifth order, is given by

$$\begin{aligned} H_{\text{eff}}=&PVRVP+PVRVRVP \\ &+PVRVRVRVP-PVR^2VPVRVP \\ &+PVRVRVRVRVP-PVRVR^2VPVRVP \\ &-PVR^2VRVPVRVP-PVR^2VPVRVRVP , \end{aligned} \tag{13}$$

where P is the projection operator projecting on the ground manifold [Eq. (12)] and $R=(1-P)/(E_0-H_0)$. H_0 contains all on-site and Coulomb interactions in Eq. (6) ($H=H_0+V$), and $E_0(=0)$ is the energy of the ground manifold when $V=0$. In the equation use is made of the fact that PVP gives a zero value since the perturbation V, equivalent to the t_{pd},t_{pp} hopping parts of the three-band Hamiltonian, will only create excited states when operating on a state in the ground manifold.

The fifth-order calculation is simplified by the following observations.

(1) Up to fifth order there are only interactions occurring between nearest-neighbor Cu spins; i.e., the effective Hamiltonian will be of the form given by Eq. (1).

(2) Most graphs resulting from Eq. (13) simply add a constant self-energy term to Eq. (1) by lowering the energy of the d orbital by the hybridization with the p states. The only remaining interaction terms are of the form

$$\sum_{\langle i,j\rangle,\sigma}d^\dagger_{i,\sigma}d^\dagger_{j,\bar\sigma}d_{j,\sigma}d_{i,\bar\sigma} , \tag{14}$$

where j is a nearest neighbor of i. The prefactor for this term determines the value of J.

(3) In the last three terms in Eq. (13), one of the intermediate states coincides with a member of the ground manifold. Since the largest of the two product members in these terms is only third order, these terms do not contribute to the exchange interaction, but only add a constant energy term to the effective Hamiltonian.

The exchange contributions up to fifth order can be divided in five categories, as depicted in Fig. 1. The

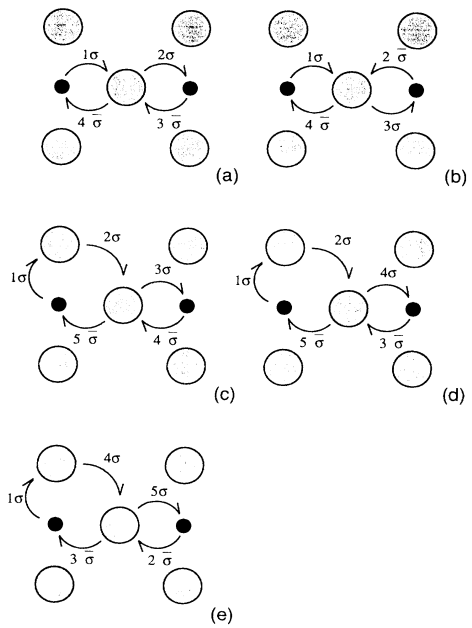

FIG. 1. Graphs of different types contributing to the (a), (b) fourth-order and (c), (d), (e) fifth-order exchange. Large circles represent oxygen, small circles copper. The numbers refer to the order in which the hoppings, represented by arrows, occur. σ and $\bar\sigma$ represent the spin of the transferred particle. Graph (c) leads to an enhancement of the U_d channel [graph (a)], graph (d) of the U_p channel [graph (b)]. Graph (e) leads to the "coherent" contribution and does not have a fourth-order counterpart.

fourth-order graphs are shown in Figs. 1(a) and 1(b). Figure 1(a) involves a doubly occupied Cu site as an intermediate state and leads to the first term in Eq. (2). Figure 1(b) involves doubly occupied oxygen sites and is responsible for the second term in Eq. (2). Note that in Fig. 1(b) the numbers 3 and 4 can be interchanged without affecting the end result, while this is not the case in Fig. 1(a). This is the reason for the extra factor of 2 in the numerator of the second term in Eq.(2).

The fifth-order exchange terms [Eq. (14)] all involve four t_{pd} hops and one t_{pp} hop. They can be divided in three categories. Figure 1(c) involves again a doubly occupied Cu site and can be compared with Fig. 1(a). Figure 1(d) is similar to Fig. 1(b) and involves a doubly occupied central oxygen site. What is important here is the number of occurrences of the different graphs in the perturbation series. If the first hop always involves the Cu site on the left, then Figs. 1(a)–1(d) have multiplicities 1, 2, 8, and 16, respectively.[30] The large multiplicity of the last two graphs demonstrates the importance of the oxygen hopping.

The last graph [Fig. 1(e)] does not have a corresponding counterpart in fourth order. This graph does not involve doubly occupied sites at all, and therefore the energy expression for this process does not involve U_d or U_p. However, it does give rise to a contribution to the superexchange, which turns out to be antiferromagnetic.

As an example, we will calculate the contribution from Fig. 1(c) in detail. The term of interest in Eq.(13) is the first fifth-order term *PVRVRVRVRVP*. Using expressions for V, R, and H_0, the expression can be written down by inspection:

$$H_{\text{eff}}=P\sum_{i,j,k,l,\sigma}(t_{pd}d^{\dagger}_{i,\sigma}p_{j,\sigma})\frac{-1}{\Delta+U_{pd}}(t_{pp}p^{\dagger}_{j,\sigma}p_{k,\sigma})$$
$$\times\frac{-1}{\Delta+U_{pd}}(t_{pd}p^{\dagger}_{k,\sigma}d_{l,\sigma})$$
$$\times\frac{-1}{U_d}(t_{pd}d^{\dagger}_{l,\bar{\sigma}}p_{k,\bar{\sigma}})\frac{-1}{\Delta+U_{pd}}(-t_{pd}p^{\dagger}_{k,\bar{\sigma}}d_{i,\bar{\sigma}})P$$
$$=\frac{4t_{pd}{}^4t_{pp}}{(\Delta+U_{pd})^3U_d}\sum_{\langle i,l\rangle,\sigma}d^{\dagger}_{i,\sigma}d^{\dagger}_{l,\bar{\sigma}}d_{l,\sigma}d_{i,\bar{\sigma}}\ . \tag{15}$$

Here i and l denote the left and right Cu sites, respectively, j is a corner oxygen, and k is the central oxygen site. In the final answer, there is a factor of 2 due to the summation over j and a factor of 2 due to the summation over neighboring pairs. Note that the parameters t_{pd} and t_{pp} are positive (by definition). Besides the graph shown in Fig. 1(c), there are three other graphs, two of which are somewhat different from this one. The difference lies in the order in which the steps occur, giving rise to different intermediate energies.

Summing all possible graphs up to fifth order (containing the fourth-order result) gives the following result for the superexchange interaction J:

$$J=J^{(4)}+J^{(5)}$$
$$=\frac{4t_{pd}^4}{(\Delta+U_{pd})^2}\left\{\frac{1}{U_d}\left[1+\frac{4t_{pp}}{\Delta+U_{pd}}+\frac{4t_{pp}}{\Delta+2U_{pd}}\right]\right.$$
$$+\frac{2}{2\Delta+U_p}\left[1+\frac{4t_{pp}}{\Delta+U_{pd}}+\frac{8t_{pp}}{2\Delta+U_{pd}}\right]$$
$$\left.+\frac{8t_{pp}}{(\Delta+2U_{pd})(2\Delta+U_{pd})}\right\}. \tag{16}$$

It is easily verified that we recover the fourth-order result [Eq. (2)] when the t_{pp} terms are omitted. Thus the terms between the round brackets represent enhancements due to the fifth-order processes. If one sets $U_{pd}=0$, this enhancement factor is $(1+8t_{pp}/\Delta)$. For $\Delta=3.5$ eV and $t_{pp}=0.65$ eV,[13] this term is ≈ 2.5. Thus t_{pp} gives rise to a large enhancement of the superexchange.

The last term in Eq. (16) corresponds to graphs of the form displayed in Fig. 1(e). This contribution will not vanish if both U_d and $U_p\rightarrow\infty$. However, the *sign* of t_{pp} will determine the sign of the superexchange when $U_d, U_p\rightarrow\infty$. This is contrary to the other fifth-order contributions, which will influence the size, but not the sign of J. Using reasonable parameters,[13] one can estimate the different contributions in Eq. (16). For $U_d=8.8$, $\Delta=3.5$, $t_{pd}=1.3$, $t_{pp}=0.65$, and $U_p=6$ (all in eV), one finds for the fourth-order exchange interaction $J^{(4)}\approx 0.25$. The last term in Eq. (16) adds ≈ 0.20 eV to this and the total fifth order $J\approx 0.82$ eV. Thus the fourth-order term accounts for less than a third of the total exchange for these parameters, and the "topological" contribution is almost as large as the fourth-order term itself. The very large value of J found here, as compared to the experimental value of ≈ 0.13 eV, demonstrates the breakdown of perturbation theory for realistic parameters.

IV. OXYGEN-BAND PERTURBATION APPROACH

In the previous section, we showed that the oxygen hopping is crucial in order to understand the magnitude as well as the different contributions to the superexchange interaction. The fifth-order expression is, however, only first order in t_{pp}. If one sets U_p and U_{pd} both equal to zero, the effect of t_{pp} can be incorporated in all orders. We can then rewrite Hamiltonian [Eq. (6)] in the form

$$H_0=\varepsilon_d\sum_{i,\sigma}d^{\dagger}_{i,\sigma}d_{i,\sigma}+\sum_{\mathbf{k},n,\sigma}\varepsilon_{\mathbf{k},n}p^{\dagger}_{\mathbf{k},n,\sigma}p_{\mathbf{k},n,\sigma}$$
$$+U_d\sum_i d^{\dagger}_{i,\uparrow}d_{i,\uparrow}d^{\dagger}_{i,\downarrow}d_{i,\downarrow}\ ,$$
$$V=\sum_{i,\mathbf{k},n,\sigma}\{V_{i,\mathbf{k},n}d^{\dagger}_{i,\sigma}p_{\mathbf{k},n,\sigma}+\text{H.c.}\}\ . \tag{17}$$

The first and third terms describe the local $3d$ orbitals and their on-site repulsion, as before. The second term describes two oxygen bands with band index $n(=\{1,2\})$, Bloch momentum $\mathbf{k}$, and energy $\varepsilon_{\mathbf{k},n}$. The perturbation V

describes the **k**-dependent coupling of the local Cu $d_{x^2-y^2}$ orbitals with the two oxygen bands and now only depends on the Cu-O hopping t_{pd}.

The two oxygen bands are

$$|\mathbf{k},1\rangle=\frac{1}{\sqrt{2}}(|\mathbf{k},x\rangle-|\mathbf{k},y\rangle)\ ,$$
$$|\mathbf{k},2\rangle=\frac{1}{\sqrt{2}}(|\mathbf{k},x\rangle+|\mathbf{k},y\rangle)\ , \tag{18}$$

with energies

$$\varepsilon_{\mathbf{k},1}=\Delta-A,\quad \varepsilon_{\mathbf{k},2}=\Delta+A\ ,$$
$$A=4t_{pp}\sin\left[\frac{k_x}{2}\right]\sin\left[\frac{k_y}{2}\right]\ . \tag{19}$$

Here the vector $|\mathbf{k},x\rangle$ ($|\mathbf{k},y\rangle$) represents the Fourier transform of the p_x (p_y) orbital. It can be shown that it is a good approximation to reduce the two bands to a single band.[34,19] However, there is no real need to do this here, and so we will keep both bands.

The **k** hybridization matrix elements can be evaluated using the real-space Hamiltonian [Eq. (6)] and the Fourier decompositions of the two wave functions in Eq. (18):

$$V_{i,\mathbf{k},1}=\left[\frac{2}{N}\right]^{1/2}t_{pd}e^{ik_xm+ik_yn-i\pi/2}\times\left[\sin\left[\frac{k_x}{2}\right]+\sin\left[\frac{k_y}{2}\right]\right]\ ,$$
$$V_{i,\mathbf{k},2}=\left[\frac{2}{N}\right]^{1/2}t_{pd}e^{ik_xm+ik_yn-i\pi/2}\times\left[\sin\left[\frac{k_x}{2}\right]-\sin\left[\frac{k_y}{2}\right]\right]\ , \tag{20}$$

where the position of the Cu atom with label i is $\mathbf{R}_i=(m,n)$ in the two-dimensional CuO_2 plane (Cu-Cu distance is set equal to 1, and m,n are integers).

The form of the Hamiltonian [Eq. (17)] implies that interactions between the Cu spins now occur only in even orders in the perturbation V. The superexchange occurs in fourth order and originates from the *PVRVRVRVP* term in Eq. (13). There are two channels. The first one involves two holes on the same Cu site. Here the first hole, say, with spin up, makes two hops via an oxygen-band state $|\mathbf{k},n\rangle$ to a second Cu site (not necessarily nearest neighbor), and then the down-spin hole makes two hops back to the original Cu site. The second process involves two oxygen holes as the intermediate state. Now the up spin from site i and down spin from site j jump into two oxygen-band states, and then the down spin hops to Cu site i and the up spin to site j. The fourth-order calculation gives[21,31–33]

$$J_{i,j}=\frac{4}{U_d}\left|\sum_{\mathbf{k},n}\frac{V_{i,\mathbf{k},n}V^*_{j,\mathbf{k},n}}{\varepsilon_{\mathbf{k},n}}\right|^2+4\sum_{\mathbf{k},n}\frac{V_{i,\mathbf{k},n}V^*_{j,\mathbf{k},n}}{(\varepsilon_{\mathbf{k},n})^2}\sum_{\mathbf{k},n}\frac{V^*_{i,\mathbf{k},n}V_{j,\mathbf{k},n}}{\varepsilon_{\mathbf{k},n}}\ . \tag{21}$$

The above-derived expressions for $V_{i,\mathbf{k},n}$ and $\varepsilon_{\mathbf{k},n}$ can be inserted in Eq. (21) to get an explicit expression for the superexchange. Equation (21) is easily evaluated numerically by sampling the Brillouin zone with a mesh of **k** points. The expression diverges when $\Delta\downarrow 4t_{pp}$, i.e., when the Cu level has the same energy as the oxygen-band edge.

The first term in the above equation can be directly compared with Anderson's superexchange theory [Eq. (5)]. This leads to an expression for $b_{i,j}$ in terms of the parameters of the three-band model:

$$b_{i,j}=\sum_{\mathbf{k},n}\frac{V_{i,\mathbf{k},n}V^*_{j,\mathbf{k},n}}{\varepsilon_{\mathbf{k},n}}\ . \tag{22}$$

In this case i and j do not have to be nearest neighbors, but can be any two Cu sites. Because $\varepsilon_{\mathbf{k},n}$ depends on the O-O hopping, $b_{i,j}$ now also depends (strongly) on t_{pp}.

The structure of the above bands is such that the Cu $d_{x^2-y^2}$ orbital mixes most strongly with the lower part of the oxygen band.[34,35,19] This can be illustrated by defining an effective oxygen level with which the Cu hybridizes:

$$\Delta^0_{\rm eff}\equiv\frac{\sum_{k,n}V_{i,\mathbf{k},n}V^*_{i,\mathbf{k},n}\varepsilon_{\mathbf{k},n}}{\sum_{\mathbf{k},n}V_{i,\mathbf{k},n}V^*_{i,\mathbf{k},n}}\ . \tag{23}$$

These sums involve simple products of sine functions and are therefore easily calculated,

$$\Delta^0_{\rm eff}=\Delta-2t_{pp}\ , \tag{24}$$

independent of the Cu index i. Since the oxygen band ranges from $\Delta-4t_{pp}$ to $\Delta+4t_{pp}$, this level lies halfway between the band center and the lower band edge, and one can expect that this will result in an enhancement of J. Note that $\Delta^0_{\rm eff}$ as defined in Eq. (23) is essentially the Δ value which enters in a calculation of the ligand-field splitting ($10Dq$), i.e., the energy difference between the Cu $d_{x^2-y^2}$ and the other d levels.

For small values of t_{pp}/Δ, we can expand the denominators in Eq. (21) in the following way:

$$\frac{1}{\varepsilon_{\mathbf{k},n}}\approx\frac{1}{\Delta}\left\{1\pm4\frac{t_{pp}}{\Delta}\sin\left[\frac{k_x}{2}\right]\sin\left[\frac{k_y}{2}\right]\right\}\ . \tag{25}$$

With this approximation the evaluation of Eq. (21) involves again only products of sine and cosine functions and can be done analytically. The result can be written in terms of an effective Δ value for the superexchange interaction. For nearest-neighbor Cu sites, one finds

$$J=\frac{4t_{pd}^4}{(\Delta^1_{\rm eff})^2}\left[\frac{1}{U_d}+\frac{1}{\Delta^1_{\rm eff}}\right]\quad(\Delta\gg t_{pp})\ , \tag{26}$$

with

$$\Delta^1_{\text{eff}}=\Delta-4t_{pp} \ . \tag{27}$$

So for both channels we find an effective Δ value which corresponds to the lower band edge. In view of Eq. (25), this is a surprising result and shows that the large value of J is not only due to the asymmetric hybridization of the Cu level with the oxygen band, but that there is an extra coherence effect between two neighboring Cu sites. The effect of t_{pp} can only be neglected when $\Delta \gg 12t_{pp}$, which is not very realistic. The approximate result [Eq. (26)] reduces to the fifth-order expression found in the previous section when we expand to lowest order in t_{pp}.

In the original theory of superexchange,[17,18] the value of J is estimated using measured crystal–ligand-field splittings, assuming $10Dq$ and $b_{i,j}$ are related by a simple proportionality constant. However, Eqs. (24) and (27) show there is no simple relation between these two quantities.

Band perturbation theory also leads to exchange interactions between Cu atoms which are further apart. In Fig. 2 we plot the ratio of two next-nearest-neighbor superexchange interactions over the nearest neighbor J. The labels (1,1) and (2,0) again refer to the position of the second Cu with respect to the first. All energies are scaled to $t_{pd}(=1)$. The ratio $t_{pp}/t_{pd}=\frac{1}{2}$ is chosen to agree with estimated values for these parameters.[12,13] Band perturbation theory predicts that the interaction becomes long range when Δ approaches $4t_{pp}$. However, this result is only valid when t_{pd} is very small. When t_{pd} is large, the cation atom will form a bound state below the bottom of the anion band, even when $\Delta<4t_{pp}$. As a result, the superexchange interaction will stay finite as well as local. In fact, one can do better than the fourth-order expression above by solving the two-hole Green function for this two-impurity problem (see Ref. 21). By looking at larger values of Δ and extrapolating the result there, one finds as a very rough estimate $J(1,1)\sim 0.1J(1,0)$. This is somewhat larger than other estimates of the next-nearest-neighbor exchange[36,16,19,13] or an experimentally deduced upper bound.[8] The other next-nearest-neighbor exchange $J(2,0)$ is very small, as can be seen in Fig. 2.

In Eq. (26) we showed that for large values of Δ/t_{pp} the band perturbation result for J can be understood in terms of an effective Δ value equal to $\Delta-4t_{pp}$. In order to make a comparison between the fourth-order expression (2) and the band perturbation result [Eq. (21)] for all values of Δ/t_{pp}, we introduce two effective charge-transfer gaps such that the nearest-neighbor superexchange is

$$J=\frac{4t_{pd}^4}{\Delta_{\text{eff}}^2}\frac{1}{U_d}+\frac{4t_{pd}^4}{(\Delta'_{\text{eff}})^3} \ . \tag{28}$$

Δ_{eff} and Δ'_{eff} are calculated explicitly by equating each contribution in Eq. (21) to the above expression for J. A plot of Δ_{eff} vs Δ is shown in Fig. 3 (solid line) together with the positions of the oxygen-band center and extrema (dotted line). A similar plot of Δ'_{eff} vs Δ is virtually indistinguishable from this, showing that $\Delta'_{\text{eff}}\approx\Delta_{\text{eff}}$. Note that the curve converges to the correct large-Δ result [Eq. (27)].

Figure 3 shows that for all values of Δ and for $U_p=0$ it is a very good approximation for the nearest-neighbor superexchange to replace the oxygen band by a single oxygen level located at energy $\Delta-4t_{pp}$, the oxygen-band edge. Since $4t_{pp}$ is estimated to be large (≈ 2.5 eV) and since the superexchange depends sensitively on this parameter [see, for instance, Eq.(2)], this evidently leads to a large correction to J.

In the previous section, we showed that the contribution arising from two holes on oxygen really consists of two contributions, one scaling as $1/U_p$ and one which is independent of the Coulomb repulsion on oxygen [see Eq. (16)]. For finite U_p the "coherent" contribution, which is independent of U_p, can never be cast in the form of Eq. (2).

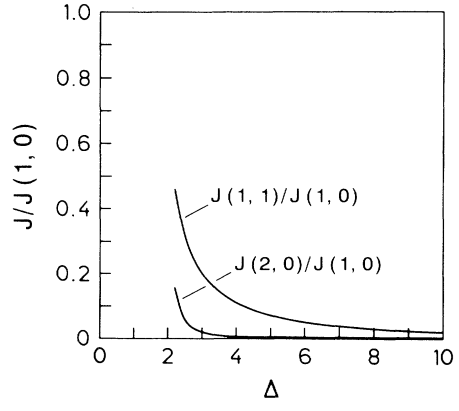

FIG. 2. Ratio between the next-nearest-neighbor superexchange interactions $J(1,1)$ and $J(2,0)$ and the nearest-neighbor superexchange $J(1,0)$ as a function of the charge-transfer energy Δ. Only the second term in Eq. (21) is calculated here. $t_{pp}=0.5t_{pd}$.

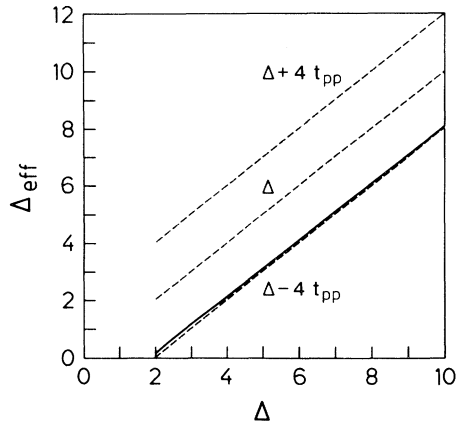

FIG. 3. Effective charge-transfer energy Δ_{eff} as a function of Δ for the $1/U_d$ term in Eq. (21). The dotted lines represent the top ($\Delta+4t_{pp}$), bottom ($\Delta-4t_{pp}$), and center (Δ) of the oxygen band. $t_{pp}=0.5t_{pd}$.

V. NUMERICAL RESULTS

In the previous sections, perturbation theory was used to derive explicit expressions for the effect of t_{pp} on the superexchange and to distinguish the various channels contributing to J. However, since neither t_{pd}/Δ nor t_{pp}/Δ are small, perturbation theory cannot be used to give a realistic estimate of the superexchange.

In this section we will compare the foregoing perturbation results with numerical calculations on finite clusters for which the superexchange constant can be obtained as the energy difference between the exact two-hole singlet and triplet ground-state energies. The two clusters we will consider here are shown in Fig. 4. The Cu_2O_7 cluster consists of two nearest-neighbor Cu sites with only nearest-neighbor oxygens. Cu_2O_{25} has a few extra shells of oxygens, and a comparison of the two results will show to what extent superexchange is determined locally. In the calculations we will use the same parameters as before, normalized to t_{pd}, unless stated otherwise.

In Fig. 5 the enhancement of the superexchange due to t_{pp} is plotted as a function of the charge-transfer energy. The solid and dashed lines correspond to Cu_2O_{25} and Cu_2O_7, respectively. The curves represent the ratio of the numerical J obtained with $t_{pp}=0.5t_{pd}$ and $t_{pp}=0$. The dotted line is the result of the fifth-order expression (16). The actual values of J obtained from Eq. (16) are much larger than the numerical results, but as can be seen from the figure, the enhancement factor is estimated quite reasonably for not too small values of Δ. So, for parameters which are reasonable for the cuprate materials, about $\frac{2}{3}$ of the exchange constant is caused by channels involving t_{pp}.

Figure 6 shows the contribution of the "coherent" channel to the total exchange. The dotted line again represent the fifth-order result and is the ratio between the last term in Eq. (16) and the total fifth-order exchange. The other two lines are the numerical data and are obtained by letting both U_d and U_p go to infinity. Again, the fifth-order term predicts roughly the right ratio between the different contributions. Comparing the two numerical results shows that the coherent term is not as locally determined as the terms involving U_d and U_p.

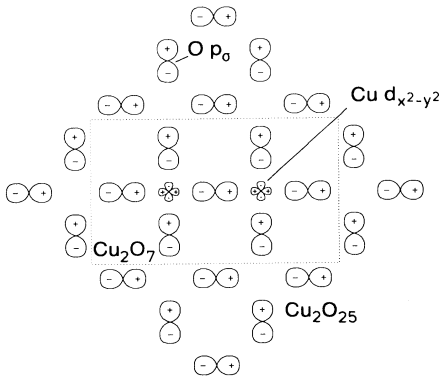

FIG. 4. Cu_2O_7 and Cu_2O_{25} clusters.

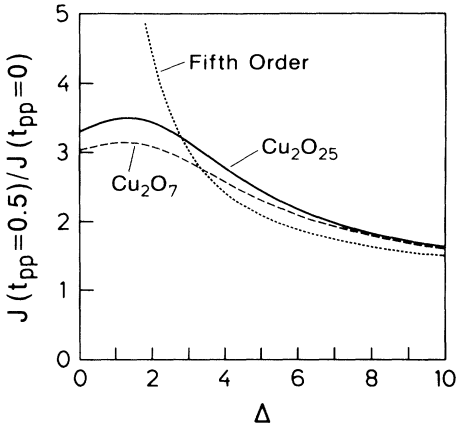

FIG. 5. Enhancement of the superexchange due to t_{pp} as a function of the charge-transfer energy. Solid line, Cu_2O_{25}; dashed line, Cu_2O_7. The dotted line is the fifth-order perturbation result $(J^{(5)}+J^{(4)})/J^{(4)}$. Parameters: $t_{pd}=1$, $t_{pp}=0.5$, $U_d=7$, and $U_p=5$.

This channel is responsible for about 25–30 % of the total exchange.

Figure 7 shows the superexchange for the two clusters as well as for the fifth-order perturbation expression. From top to bottom, the curves correspond to $t_{pp}=0.5$, $t_{pp}=0$, and $t_{pp}=-0.5$. Note that for $t_{pp}=0$ the two clusters give the same result. The curve for $t_{pp}=0.5$ gives an estimate of J of about 0.2 eV. Considering that we neglected intersite exchange interactions (see Sec. II), this is not unreasonable. A comparison of the fifth-order results with the numerical curves shows that perturbation theory converges only for very large values of Δ ($\Delta/t_{pd}\geq 7$). The fifth-order expression for $t_{pp}=0$ is identical to the usual fourth-order result, and so the two dotted curves give a comparsion between fourth- and fifth-order perturbation theory. Comparing the numerical re-

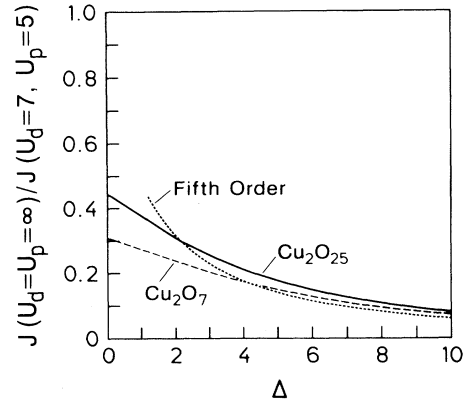

FIG. 6. Contribution of the "coherent" exchange to the total antiferromagnetic exchange as a function of the charge-transfer energy. Solid line, Cu_2O_{25}; dashed line, Cu_2O_7. The dotted line is the fifth-order perturbation result. Parameters: $t_{pd}=1$, $t_{pp}=0.5$, $U_d=7$, and $U_p=5$.

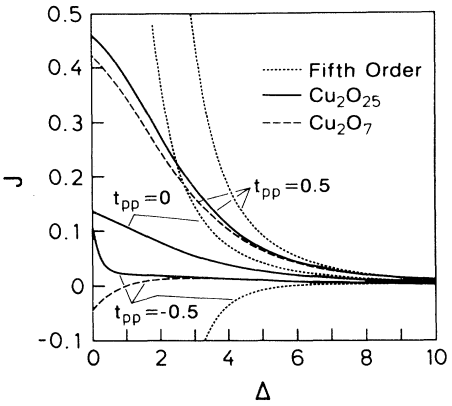

FIG. 7. Total exchange interaction as a function of the charge-transfer energy. Solid lines, Cu_2O_{25}; dashed lines, Cu_2O_7. The dotted lines are the fifth-order perturbation result. The top three curves correspond to $t_{pp}=0.5$, the middle three curves correspond to $t_{pp}=0$, and the bottom three curves correspond to $t_{pp}=-0.5$. Parameters: $t_{pd}=1$, $U_d=7$, and $U_p=5$.

sults with the fourth-order curve shows that in this case the results are much worse, and convergence to the exact result occurs only for extremely large values of Δ. The ratios between the top and middle curves were already compared in Fig. 5.

The lower three curves show what happens if the sign of the oxygen-oxygen hopping is reversed. In this case the two clusters predict an almost vanishing exchange constant, and the fifth-order perturbation expression even predicts a ferromagnetic coupling between the spins. This is due to two effects. In the first place, the two contributions connected with a doubly occupied site are strongly reduced [but still antiferromagnetic; see Eq. (16)]. Second, the sign of the coherent term is determined by the sign of t_{pp}, and therefore this term leads to a ferromagnetic coupling.

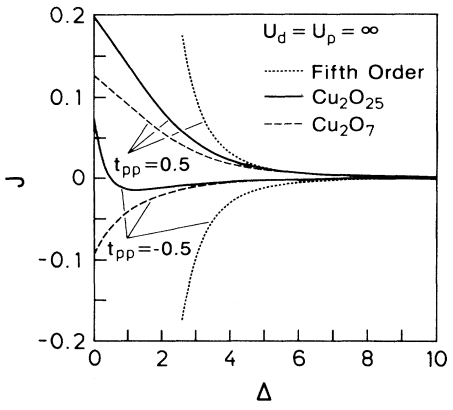

FIG. 8. Exchange interaction for U_d and $U_p\rightarrow\infty$ ("coherent" exchange only) as a function of the charge-transfer energy. Solid lines, Cu_2O_{25}; dashed lines, Cu_2O_7. The dotted lines are the fifth-order perturbation result. The top three curves correspond to $t_{pp}=0.5$, and the bottom three curves correspond to $t_{pp}=-0.5$.

The effect of reversing the sign of t_{pp} is shown in Fig. 8 for the "coherent" exchange contribution only. The dotted lines come from the last term in Eq. (16), and the other two curves show the numerical result for U_d and $U_p\rightarrow\infty$. For negative t_{pp}, both clusters now give a ferromagnetic result (for not too small values of Δ).

The important aspect here is not really the sign of t_{pp}, but the sign of the product of the three hopping parameters in the Cu-O-O triangles. It is easy to show that the three-band Hamiltonian is invariant under a change of any two of these three signs. We checked this explicitly for the Cu_2O_{25} cluster by keeping $t_{pp}=0.5$ and changing the sign of the Cu-O hopping to the oxygen p_y orbital only (the Cu orbital now behaves as an s orbital). The result for J is found to be identical to the curve in Fig. 7 for $t_{pp}=-0.5$.

To investigate the effect of U_{pd} on the superexchange, we repeated the above calculations for $U_{pd}=1$. The two resulting figures were found to be almost identical to Figs. 7 and 8, provided Δ is replaced by $\Delta+U_{pd}$. Thus the effect of U_{pd} can be interpreted in terms of a simple shift of the charge-transfer energy Δ [see Eq. (16)].

As already mentioned above, the "coherent" exchange is more a delocalized effect than the channels involving a doubly occupied site. This gives rise to the difference in the two numerical curves in Fig. 8. This is easily understood since the probability that the two holes will meet on an oxygen site far away from the central oxygen is very small. The total coherent contribution can be seen as a sum of a contribution due to the Cu-O-O triangles, the sign of which depends on the sign of the hopping-matrix elements and a smaller contribution due to the square oxygen lattice, which is always antiferromagnetic. A comparison of the numerical results for the two clusters illustrates this effect. For small values of Δ, the value of J for the Cu_2O_{25} cluster is always more positive than for the Cu_2O_7 cluster. This suggests that, for t_{pp} negative, the effect of the other Cu neighbors, i.e., those neglected in the Cu_2O_{25} cluster, is a ferromagnetic contribution to J. To check this idea, we introduced six Cu sites in the cluster. These were treated as empty, but with an on-site energy U_d (due to the frozen "spectator" spin) and with a hybridization t_{pd}. The calculation indeed shows the predicted effect, but the resulting ferromagnetic correction is only very small.

VI. CONCLUSIONS

In Secs. III and IV we demonstrated the importance of the oxygen-oxygen hopping for the exchange interaction by means of perturbation theory. By writing explicit expressions for J, we could distinguish three different contributions to the exchange interaction. In the last section, we compared the perturbation results with exact numerical diagonalizations of small clusters. It was found that the perturbation approach predicts approximately the correct ratios between the different contributions, but cannot be used to give a quantitative estimate for the superexchange unless Δ/t_{pd} is very large.

In a previous paper,[19] we introduced a cell perturbation method (see also Refs. 37 and 38). In this approach the CuO_2 planes are partitioned into CuO_4 units. The three-band Hamiltonian is then written in term of an intercell and intracell part. The intracell part is subsequently solved exactly, which treates a large part of the *p-d* and *p-p* hybridization up to infinite order. Starting from this set of cell eigenstates, one can then treat the smaller intercell part of the Hamiltonian in perturbation theory. The superexchange interaction now occurs already in second order. The superexchange constant J in this method does not diverge when $\Delta \rightarrow 0$, and we showed that there is good agreement between this method and numerical results, in contrast to the perturbation methods used above. Note that the fact that a superexchange constant can be calculated for small values of Δ does not imply that the system remains an antiferromagnetic (AFM) insulator down to $\Delta = 0$ since an insulator-metal (Mott) transition will occur at some finite Δ.

In this paper we calculated the superexchange for different values of t_{pp} and we also found that t_{pp} gives rise to a strong enhancement of J [see Fig. 5 and Eq. (27) in Ref. 19]. Note, however, that the calculations were done with $U_p = 0$ and that therefore this enhancement should again be interpreted as consisting of an enhancement of the conventional $1/U$ channels, as well as a U-independent coherent part. In the cell method, much of the effect of t_{pp}, including the coherent contributions, is contained in the intracell solutions. This is because the intermediate two-hole cell wave functions also contain components where the two holes are on different oxygen sites.

In a recent paper, Aronson *et al.* have measured pressure-dependent Raman scattering on antiferromagnetic La_2CuO_4.[39] They plotted $\ln J$ vs $\ln r$, where r is the Cu-O distance, and found a scaling $J \sim r^{-6.4}$ and point out that this exponent is much smaller than can be expected from the fourth-order perturbation expression. This may be estimated by assuming $t_{pd} \sim r^{-3 \pm 0.5}$ (see, for example, Ref. 40), which would predict that $J \sim t_{pd}^4 \sim r^{-12}$. (Other parameters such as Δ can be expected to scale with a much lower exponent). To make a more realistic estimate, we calculated J numerically as a function of t_{pd} assuming $t_{pp} \sim t_{pd}^{2/3}$ [i.e., $t_{pp} \sim r^{-2}$ (Ref. 40)] and neglected the (small) variation with r of the other parameters. For the parameters mentioned in Sec. III, we find $J \sim t_{pd}^{2.3}$ (i.e., $J \sim r^{-6.9}$), in good agreement with experiment. This again illustrates the poor description obtained from perturbation theory.

The aim of this paper has been to identify the various contributions to the AFM superexchange interaction in the insulating parent compounds of the high-T_c superconductors and to estimate their relative magnitudes. The main results may be summarized as follows.

(1) The O-O hopping t_{pp} is crucial for an understanding of the large value of J. It leads to an overall enhancement of J of about a factor of 3.

(2) It is well known that the copper $d_{x^2-y^2}$ level hybridizes with the lower part of the oxygen band [see Eq. (24)], and it would seem reasonable to explain the effect of t_{pp} on the superexchange in this way. However, in Sec. IV we showed that the effect of oxygen hopping is much stronger than this and is more accurately described by an effective charge-transfer energy which coincides with the oxygen-band edge.

(3) The contributions to the superexchange can be divided into five terms. The first and second are the two conventional channels, one involving double occupancy of Cu and one involving a doubly occupied central oxygen site. The third and fourth terms cause an enhancement of the first two terms due to the oxygen hopping. The enhancement factor is large: approximately 2.5.

(4) The fifth contribution is of an entirely different nature. It does not involve doubly occupied sites and does not vanish when both U_d and U_p are infinite. The singlet and triplet Hilbert spaces in this case have the same dimension, and the absolute values of the matrix elements are the same. We called this the "coherent" term since the singlet-triplet energy difference is due to the signs of the matrix elements and therefore depends on the coherence of the singlet and triplet wave functions. This term can be antiferromagnetic as well as ferromagnetic, depending on the topology of the cation-anion lattice. It cannot be neglected, as it is almost as large as the first two terms together. That the effect is so large is precisely due to the fact that it does not involve U.

(5) The coherent channel is a consequence of the extra degrees of freedom formed by the oxygen states, and the CuO_2 planes in this case are more appropriately described as a $\frac{1}{6}$-filled than a $\frac{1}{2}$-filled band system. In a single-band Hubbard model, such extra degrees of freedom are not present, and therefore there is no coherent contribution in this model.

(6) Perturbation theory converges very slowly and should not be used to make a realistic estimate. The fifth-order expression approximates to the numerical result only for $\Delta / t_{pd} \geq 7$. For the fourth-order expression, things are much worse. The reasonable estimate of J obtained from this fourth-order expression is therefore purely coincidental (see Fig. 7). In this respect the cell perturbation method proves to be a promising alternative.

(7) In the three-center cation-anion-cation (CAC) model, the large AFM kinetic exchange is caused by the 180° CAC angle and the large hybridization parameter t_{pd}^2 / Δ. The large enhancement of J is, however, caused by another structural unit, namely, the Cu-O-O triangles. Changing the sign of one of the hopping parameters in these triangles leaves the normal fourth-order exchange unaltered (first two terms), but results in a drastic reduction of the total J. Since we neglected more direct ferromagnetic exchange integrals in our starting Hamiltonian (see Sec. II), such a sign change could well result in a ferromagnetic coupling.

ACKNOWLEDGMENTS

This investigation was supported by the European Community under the SCIENCE program for collaborative research (Contract No. SCI-0222-C).

*Present address: Max-Planck-Institut für Festkörperforschung, Heisenbergstrasse 1, 70563 Stuttgart, Federal Republic of Germany.

[1]*High Temperature Superconductivity,* edited by K. S. Bedell, D. Coffey, D. E. Meltzer, D. Pines, and J. R. Schrieffer (Addison-Wesley, Redwood City, CA, 1990).
[2]S. Chakravarty, in *High Temperature Superconductivity* (Ref. 1), p. 136.
[3]E. Manousakis, Rev. Mod. Phys. **63**, 1 (1991).
[4]G. Aeppli *et al.*, Phys. Rev. Lett. **62**, 2052 (1989).
[5]Y. Endoh *et al.*, Phys. Rev. B **37**, 7443 (1988); K. Yamada *et al.*, *ibid.* **40**, 4557 (1989).
[6]R. R. P. Singh, P. A. Fleury, K. B. Lyons, and P. E. Sulewski, Phys. Rev. Lett. **62**, 2736 (1989).
[7]T. A. Kaplan, S. D. Mahanti, and H. Chang, Phys. Rev. B **45**, 2565 (1992).
[8]S. M. Hayden, G. Aeppli, R. Osborn, A. D. Taylor, T. G. Perring, S.-W. Cheong, and Z. Fisk, Phys. Rev. Lett. **67**, 3622 (1991).
[9]H. J. Schmidt and Y. Kuramoto, Physica C **167**, 263 (1990).
[10]E. R. Gagliano, C. A. Balseiro, and M. Avignon, Europhys. Lett. **12**, 259 (1990).
[11]V. J. Emery, Phys. Rev. Lett. **58**, 2794 (1987); C. M. Varma, S. Schmidt-Rink, and E. Abrahams, Solid State Commun. **62**, 681 (1987).
[12]A. K. McMahan, R. M. Martin, and S. Satpathy, Phys. Rev. B **38**, 6650 (1988); M. S. Hybertsen, M. Schluter, and N. E. Christensen, *ibid.* **39**, 9028 (1989); L. F. Mattheiss and D. R. Hamann, *ibid.* **40**, 2217 (1989).
[13]H. Eskes, G. A. Sawatzky, and L. F. Feiner, Physica C **160**, 424 (1989).
[14]Y. Ohta, T. Tohyama, and S. Maekawa, Phys. Rev. Lett. **66**, 1228 (1991); S. Maekawa, J. Inoue, and T. Tohyama, in *Strong Correlation and Superconductivity,* edited by H. Fukuyama, S. Maekawa, and A. P. Malozemoff, Springer Series in Solid-State Sciences Vol. 89 (Springer-Verlag, Berlin, 1989), p. 66.
[15]E. B. Stechel and D. R. Jennison, Phys. Rev. B **38**, 4632 (1988).
[16]J. F. Annett, R. M. Martin, A.K. McMahan, and S. Satpathy, Phys. Rev. B **40**, 2620 (1989).
[17]P. W. Anderson, Phys. Rev. **115**, 2 (1959); **79**, 350 (1950).
[18]P. W. Anderson, Solid State Phys. **14**, 99 (1963); in *Magnetism,* edited by G. T. Rado and H. Suhl (Academic, New York, 1963), Vol. I, p. 25.
[19]J. H. Jefferson, H. Eskes, and L. F. Feiner, Phys. Rev. B **45**, 7959 (1992).
[20]T. Kostyrko, Phys. Rev. B **40**, 4596 (1989).
[21]W. Geertsma, Ph.D. thesis, University of Groningen, the Netherlands, 1979; Physica B **164**, 241 (1990).
[22]B. E. Larson, K. C. Hass, and H. Ehrenreich, Solid State Commun. **56**, 347 (1985).
[23]J. Zaanen, Ph.D. thesis, University of Groningen, the Netherlands, 1986; J. Zaanen and G. A. Sawatzky, Can. J. Phys. **65**, 1262 (1987).
[24]Z.-X. Shen *et al.*, Phys. Rev. B **36**, 8414 (1987).
[25]P. Prelovsek, Phys. Lett. A **126**, 287 (1988).
[26]J. Zaanen and A. M. Oleś, Phys. Rev. B **37**, 9423 (1988).
[27]M. Ogata and H. Shiba, J. Phys. Soc. Jpn. **57**, 3074 (1988).
[28]J. H. Jefferson, J. Phys. C **21**, L193 (1988).
[29]I. Lindgren and J. Morrison, *Atomic Many-Body Theory* (Springer-Verlag, Berlin, 1986), and references therein.
[30]This is not completely correct, since, as we shall see, graphs belonging to the categories as defined by which site is doubly occupied do not all give the same contribution.
[31]C. E. T. Gonçalves da Silva and L. M. Falicov, J. Phys. C **5**, 63 (1972).
[32]J. L. Shen, J. H. Xu, C. S. Ting, and T. K. Lee, Phys. Rev. B **42**, 8728 (1990).
[33]D. Ihle and M. Kasner, Phys. Rev. B **42**, 4760 (1990).
[34]J. F. Annett and R. M. Martin, Phys. Rev. B **42**, 3929 (1990).
[35]H. Eskes and G. A. Sawatzky, Phys. Rev. B **44**, 9656 (1991).
[36]M. S. Hybertsen, E. B. Stechel, M. Schluter, and D. R. Jennison, Phys. Rev. B **41**, 11 068 (1990).
[37]H.-B. Schüttler and A. J. Fedro, Phys. Rev. B **45**, 7588 (1992).
[38]R. Hayn, V. Yushankhai, and S. Lovtsov (unpublished); S. V. Lovtsov and V. Y. Yushankhai, Physica C **179**, 159 (1991).
[39]M. C. Aronson *et al.*, Phys. Rev. B **44**, 4657 (1991).
[40]W. A. Harrison, *Electronic Structure and the Properties of Solids* (Freeman, San Francisco, 1980).